

Decoding the neural basis of olfactory dysfunction: a multimodal MRI study in CRS-OD

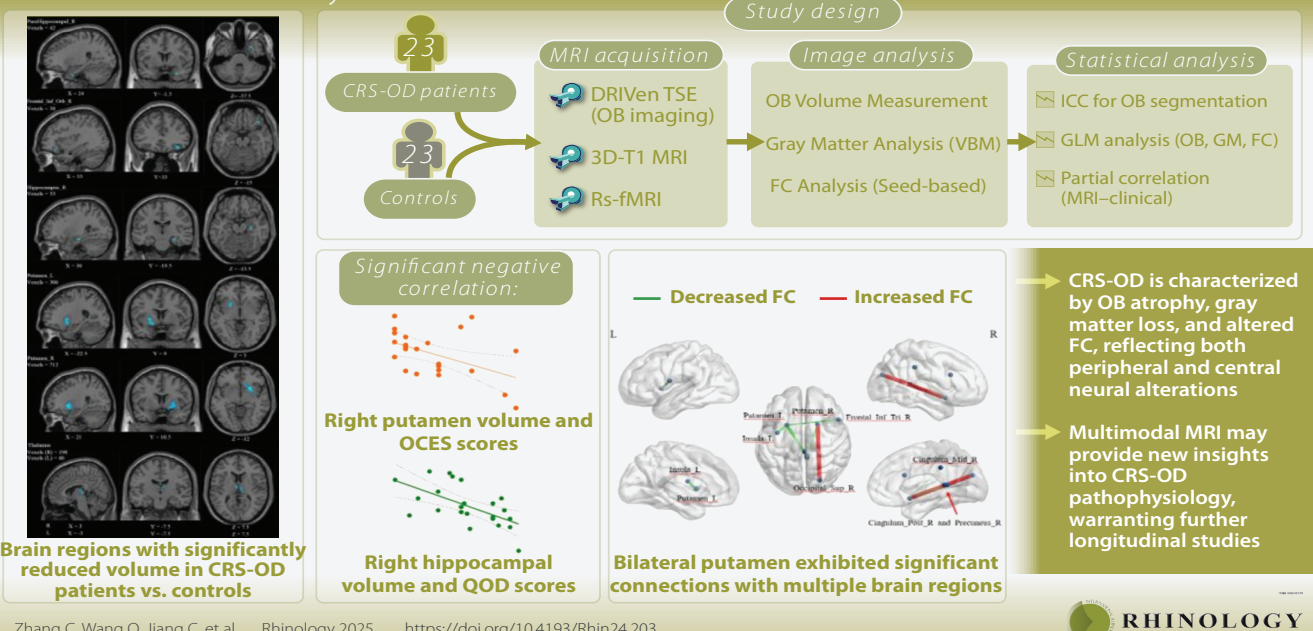
Chao Zhang¹, Qi Wang¹, Canran Jiang¹, Zhenni Tian³, Jingyun Sha¹,
Xiao Wang¹, Wanrong Zhou¹, Teng Cui¹, Yunpeng Zang^{2,*}, Kai Xu^{1,*}

Rhinology 64: 2, 0 - 0, 2026

<https://doi.org/10.4193/Rhin25.096>

Decoding the neural basis of olfactory dysfunction

A multimodal MRI study in CRS-OD



Zhang C, Wang Q, Jiang C, et al. Rhinology 2025. <https://doi.org/10.4193/Rhin24.203>

Abstract

Background: Chronic rhinosinusitis with olfactory dysfunction (CRS-OD) affects both peripheral and central olfactory pathways. Persistent olfactory loss may induce neuroplastic changes in brain regions involved in olfactory processing. We hypothesized that CRS-OD is associated with gray matter atrophy in olfactory-related regions, accompanied by alterations in global functional connectivity as a manifestation of compensatory or maladaptive reorganization. To test this, we performed voxel-based morphometry (VBM) to identify gray matter differences, followed by seed-based functional connectivity (FC) analysis using the altered regions. **Methodology:** We prospectively recruited 23 CRS-OD patients and 23 healthy controls (HCs). All patients presented with persistent olfactory dysfunction lasting 6 to 240 months. All participants underwent MRI scanning at the same time point. Olfactory function was assessed in CRS-OD patients using the Threshold-Discrimination-Identification (TDI) test, the Questionnaire of Olfactory Disorders (QOD), and the Olfactory-Evoked Cognitive Score (OCES). MRI analyses included VBM, FC, and olfactory bulb volume on DRIVen Equilibrium turbo spin echo (TSE) images. **Results:** CRS-OD patients exhibited significantly reduced olfactory bulb (OB) volumes compared to HCs and gray matter atrophy in the inferior frontal orbital gyrus, parahippocampal gyrus, hippocampus, thalamus, and putamen. FC analysis revealed decreased connectivity in sensory-integration networks and increased FC in the superior occipital gyrus, suggesting compensatory reorganization. **Conclusions:** CRS-OD is characterized by OB atrophy, gray matter atrophy, and disrupted FC, reflecting both peripheral and central neural alterations. Multimodal MRI may provide new insights into CRS-OD pathophysiology, warranting further longitudinal studies.

Key words: chronic rhinosinusitis, olfaction disorders, smell, rhinosinusitis

Introduction

Olfactory dysfunction (OD) represents one of the most common and distressing manifestations of chronic rhinosinusitis (CRS), with substantial impact on patients' quality of life and daily functioning⁽¹⁾. The prevalence of CRS-OD varies between 48% and 83%, contingent upon the diagnostic criteria employed⁽²⁻⁴⁾. In addition to impairing odor perception, CRS-OD significantly impacts patients' safety, nutrition, and emotional well-being⁽⁴⁾. However, the pathophysiological mechanisms of CRS-OD remain incompletely understood, particularly concerning the interplay of peripheral damage, impaired neurogenesis, and central nervous system involvement. The European Position Papers on Olfactory Dysfunction have comprehensively outlined the etiologies, and mechanisms of olfactory loss, emphasizing the interplay of obstructive processes, neuroepithelial inflammation, and possible central neural alterations in CRS-OD^(5, 6). In line with these frameworks, studies have further characterized the peripheral inflammatory mechanisms contributing to CRS-OD. Nasal inflammation and epithelial remodeling hinder odorant access to olfactory receptors, while chronic inflammation can cause direct damage to olfactory sensory neurons and impair neurogenesis⁽⁷⁾. Recent studies have demonstrated that chronic inflammation impairs olfactory neurogenesis by disrupting horizontal basal cells (HBCs), the neural stem cells for olfactory sensory neurons. Persistent NF-κB signaling drives HBCs into an immune-activated state, suppressing regeneration and amplifying mucosal inflammation, leading to sustained olfactory dysfunction⁽⁸⁾. Inflammatory injury also induces immune cell infiltration and elevated pro-inflammatory cytokines, such as TNF-α and IL-1β, which promote epithelial damage, neuronal loss, and impaired olfactory function⁽⁹⁻¹¹⁾. These peripheral inflammatory mechanisms may underlie or contribute to the structural and functional alterations observed in central olfactory pathways.

Beyond peripheral olfactory structures, CRS-OD is also associated with alterations in higher-order brain regions involved in olfactory processing, including the orbitofrontal cortex, insula, and hippocampus^(15, 16). In addition, olfactory processing is thought to include multiple brain regions involved in broader sensory integration, emotional regulation, and cognitive control. The putamen integrates olfactory and sensorimotor information⁽¹⁷⁾, the insular cortex contributes to sensory integration and emotional regulation⁽¹⁸⁾, the cingulate cortex is involved in cognitive and affective processing⁽¹⁹⁾, and the precuneus is involved in higher-order sensory integration⁽²⁰⁾. Neuroimaging studies revealed structural and functional changes in these regions, correlating with the severity of olfactory impairment, such as the orbitofrontal cortex and insula⁽¹²⁻¹⁴⁾.

In particular, functional connectivity (FC) abnormalities related to olfactory processing have received increasing attention in CRS-OD studies. FC refers to the temporal synchronization of

neural activity between anatomically distinct brain regions at rest, reflecting functional interactions between specific brain areas or networks⁽²¹⁻²³⁾. In CRS-OD, abnormalities in FC have been observed within sensory-integration networks, including the parahippocampal gyrus, frontal gyrus, and cerebellum, suggesting involvement of not only olfactory-specific regions but also broader neural systems related to sensory integration and cognitive processing^(3, 24).

Despite these advancements, significant gaps remain in understanding how CRS-OD influences brain structure and function, hindering the development of effective management strategies⁽²⁵⁾.

Previous studies have made important contributions to understanding brain alterations in CRS-OD by applying single-modality MRI techniques, such as brain structure or FC analyses^(12, 26). Building upon these foundations, comprehensive multimodal investigations may offer further insights into the complex central mechanisms underlying olfactory dysfunction.

This study was designed to test the hypothesis that CRS-OD involves both peripheral olfactory bulb (OB) atrophy and central alterations, including gray matter atrophy and FC changes within olfactory-related brain regions. Multimodal MRI allows a comprehensive assessment of structural and functional brain changes and may provide new insights into the central mechanisms of CRS-OD.

Materials and methods

Study design

This prospective, single-center study was conducted between May 2023 and May 2024 at the Affiliated Hospital of Xuzhou Medical University. The study protocol was approved by the Institutional Review Board (Ethics No. XYFY2023-KL085-02), and written informed consent was obtained from all participants.

Subjects

A total of 23 patients with chronic rhinosinusitis with CRS-OD and 23 age- and sex-matched healthy controls (HCs) participated in this study. CRS-OD patients were clinically diagnosed by otorhinolaryngologists based on clinical symptoms and endoscopic, following the European Position Paper on Rhinosinusitis and Nasal Polyps (EPOS) guidelines⁽²⁷⁾. Inclusion criteria for the CRS-OD group were: 1) a confirmed diagnosis of CRS-OD persisting for at least 12 weeks; Olfactory function was classified based on TDI scores as follows: normosmia (TDI > 31.0), mild dysosmia (28.5 ≤ TDI ≤ 31.0), moderate dysosmia (16.5 ≤ TDI < 28.5), and severe dysosmia/anosmia (TDI < 16.5)^(28, 29); 2) olfactory dysfunction verified by the Threshold-Discrimination-Identification (TDI) test; and 3) no history of endoscopic sinus surgery (ESS). At the time of MRI acquisition, all patients underwent olfactory function assessment using the TDI scale to ensure consistency between clinical and imaging data. In addition, the duration of

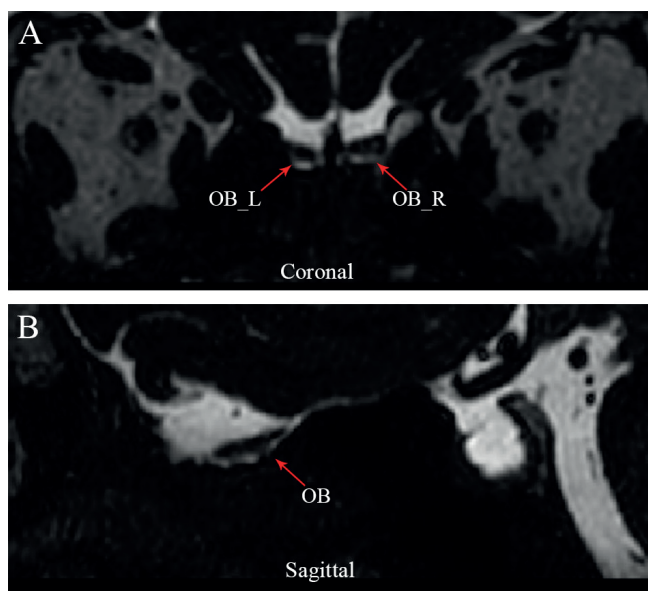


Figure 1. MRI of the Olfactory Bulb Using DRIVen Equilibrium Turbo Spin Echo (TSE) Sequence. A) Coronal view showing bilateral olfactory bulbs (red arrows). B) Sagittal view highlighting the olfactory bulb on one side (red arrow).

OB was recorded at enrollment for each patient, ranging from 6 to 240 months. All patients had previously received intranasal corticosteroid treatment as part of their standard CRS management prior to enrollment. Exclusion criteria included significant comorbid conditions, psychiatric disorders, traumatic brain injury, or other causes of olfactory dysfunction. All patients underwent fMRI along with clinical assessments, including the Questionnaire of Olfactory Disorders (QOD), Olfactory-Evoked Cognitive Score (OECS), and TDI test.

For the HC group, inclusion criteria were: no evidence of olfactory dysfunction (e.g., due to allergic rhinitis, nasal polyps, or chronic sinusitis) as confirmed by an olfaction evaluation; no other conditions affecting olfaction; and no factors that could interfere with the study, such as a history of mental illness or neurological disorders. Exclusion criteria for HCs included the use of medications affecting olfaction, as well as smoking, alcoholism, or drug dependence. All HCs underwent fMRI examinations.

Image acquisition

The acquisition of MRI data for all participants was performed at the Department of Radiology, Affiliated Hospital of Xuzhou Medical University, using a Philips Elition 3.0T MR scanner. The scanning parameters were specified as follows: 1) High-resolution structural data were acquired using a three-dimensional whole-brain volume imaging sequence (3DT1WI-BRAVO), covering the region from the axis (C2) to the top of the head. The parameters included a repetition time (TR) of 7.0 ms, an echo time (TE) of 3.0

ms, a field of view (FOV) of 256 mm × 256 mm, 192 slices, and a voxel size of 1.0 mm × 1.0 mm × 1.0 mm. 2) Resting-state BOLD functional data were obtained using an echo-planar imaging (EPI) sequence, encompassing the entire brain. The scanning baseline was aligned parallel to the anterior-posterior commissure line, with 36 slices acquired, a matrix size of 64 × 64, a slice thickness/spacing of 3 mm/1 mm, a TR of 2000 ms, a TE of 30 ms, a flip angle of 90°, and a total of 185 time points. 3) For olfactory bulb imaging, the DRIVen Equilibrium turbo spin echo (TSE) sequence was employed, with a TR of 4000 ms, a TE of 111 ms, an FOV of 200 mm × 200 mm × 80 mm, 40 slices, and a voxel size of 0.6 mm × 0.6 mm × 2 mm.

Data analysis

Brain structure preprocessing

Voxel-based morphometry (VBM) analysis was employed to examine differences in gray matter between the two groups. This analysis was executed using Statistical Parametric Mapping (SPM) software, specifically version SPM12.0, operating on MATLAB (version R2020a, MathWorks, Natick, MA, USA). The preprocessing protocol involved segmenting images into gray matter, white matter, and cerebrospinal fluid (CSF), followed by spatial normalization to the Montreal Neurological Institute (MNI) template space. Subsequently, the gray matter images were smoothed with an isotropic Gaussian kernel of 6 mm full width at half maximum (FWHM) to improve the signal-to-noise ratio and accommodate inter-subject anatomical variability.

Olfactory bulb volume measurement

The olfactory bulb volume was segmented manually using ITK-SNAP software (<http://www.itksnap.org/pmwiki/pmwiki.php>) based on the DRIVen Equilibrium TSE sequence (Figure 1). The OB boundaries were identified visually and delineated slice-by-slice by trained raters. Two residents, each with two years of professional experience, independently delineated the olfactory bulb structure to ensure measurement reliability.

Functional data preprocessing

Resting-state functional MRI (rs-fMRI) data were preprocessed and analyzed using the DPARSF toolbox (version 5.4, Data Processing Assistant for Resting-State fMRI) within the MATLAB environment (MathWorks, Natick, MA, USA) ⁽³⁰⁾. The preprocessing protocol encompassed several steps: conversion of raw DICOM images to NIFTI format, slice timing correction with the middle slice as a reference, and head motion correction by realigning each volume to the mean image. Participants exhibiting head motion equal to or exceeding 2.0 mm or 2.0° were excluded from further analysis. Friston's 24 head motion parameters were documented for nuisance regression purposes. Functional images were coregistered to T1-weighted structural images, which were subsequently segmented into gray matter, white

Corrected Proof

Neural basis of olfactory dysfunction in CRS-OD

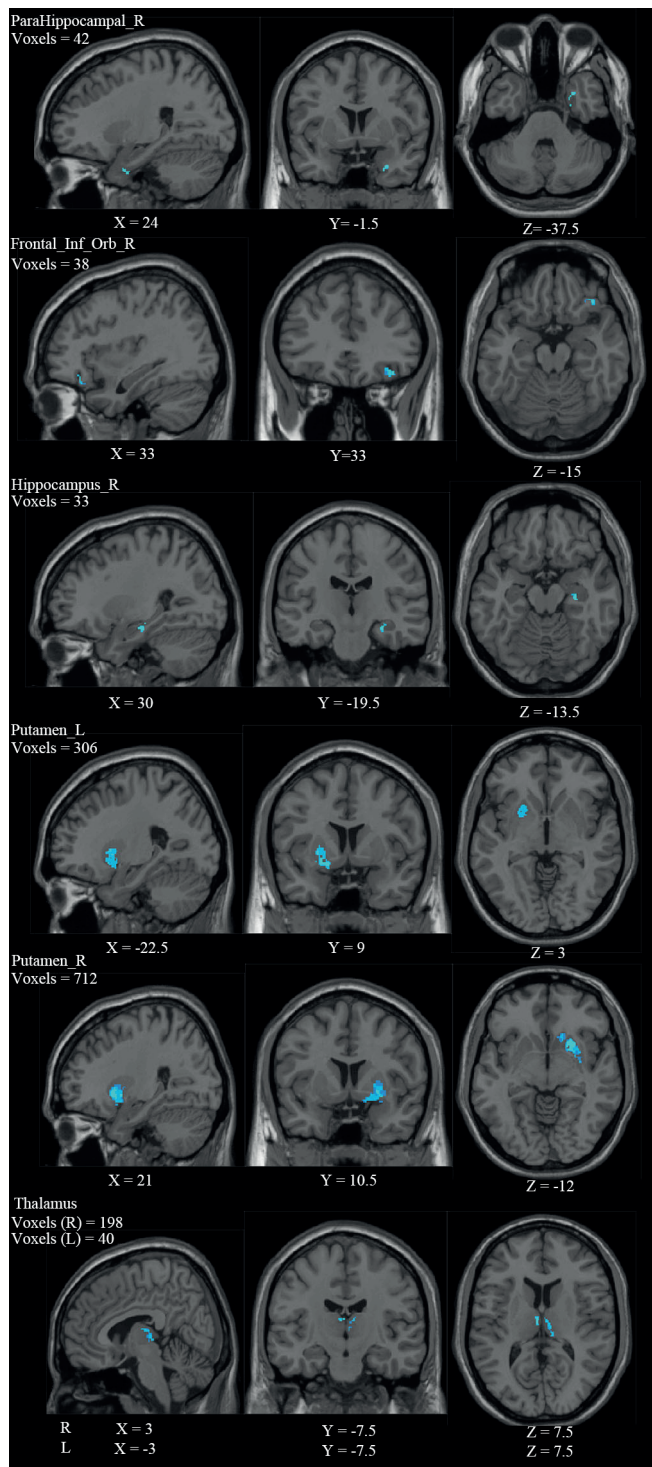


Figure 2. Brain Regions with Significant Volume Reduction in CRS-OD Patients Compared to HCs. Brain areas exhibiting significant volume reduction in CRS-OD patients are shown ($p < 0.05$, FDR-corrected). Significant clusters are shown in sagittal, axial, and coronal views. The peak MNI coordinates (x, y, z) and corresponding cluster sizes (number of voxels) are labeled for each region. CRS-OD, Chronic rhinosinusitis with olfactory dysfunction; HCs, Healthy controls.

matter, and cerebrospinal fluid (CSF). The DARTEL algorithm was employed to normalize images to the Montreal Neurological Institute (MNI) template, and functional images were resampled to a voxel size of $3 \times 3 \times 3$ mm. Spatial smoothing was conducted using a Gaussian kernel with a full width at half maximum (FWHM) of 6 mm, followed by the application of a band-pass filter (0.01–0.1 Hz). Nuisance covariates, including head motion, global signal, white matter, and CSF signals, were regressed out. Rigorous quality control checks were implemented to ensure data integrity, resulting in the exclusion of participants with artifacts.

FC analysis was performed using seed regions selected based on the structural alterations identified in our VBM results. The mean time series from each seed region were correlated with all brain voxels to produce whole-brain connectivity maps, with Pearson correlation coefficients subsequently Fisher Z-transformed for statistical analysis.

Statistical analysis

All statistical analyses were performed using MATLAB R2020a. Statistical significance was determined at a p -value < 0.05 or an adjusted p -value < 0.05 using the Benjamini-Hochberg correction. Group comparisons were conducted using Student's t-test and the Mann-Whitney U test, while the Chi-square test was employed for categorical data analysis. Inter-rater reliability was evaluated using the intraclass correlation coefficient (ICC), categorized as low (0.00–0.40), moderate (0.41–0.75), or high (0.76–1.00). Group comparisons of OB volumes, gray matter volumes, and FC were performed using general linear models (GLM), with group (CRS-OD vs. HCs) as the independent variable and age and sex included as covariates. The false discovery rate (FDR) correction was applied to control for multiple comparisons ($p < 0.05$). Partial correlation analysis, adjusting for age and sex, was used to examine correlations between clinical scores, olfactory bulb properties, and MRI measures, with FDR correction applied ($p < 0.05$).

Results

Demographic and clinical characteristics

The demographic characteristics of participants are summarized in Table 1. CRS-OD patients had a median age of 38 years (range: 35–52), including 14 males (60.87%) and 9 females (39.13%). The median scores for the QOD, OCES, and TDI test were 31.00 [14.50, 43.00], 4.00 [2.00, 7.00], and 31.00 [14.50, 43.00], respectively. In comparison, the HC group had a median age of 50 years (range: 29–52), with 12 males (52.17%) and 11 females (47.83%). No significant differences were found in age or sex distribution between the groups ($p > 0.05$). The median duration of OD was 24 months (range 6–240 months). Seventeen CRS-OD patients and 17 HCs underwent DRIVen Equilibrium Turbo Spin Echo sequences for OB volume assess-

Table 1. Demographics of all subjects.

Variable	Overall N = 46 ¹	HC N = 23 (50%) ¹	CRS-OD N = 23 (50%) ¹	p-value ²
Age	41.00 [29.25, 52.50]	50.00 [29.00, 52.00]	38.00 [35.50, 52.50]	0.904
Sex				0.766
Male	26 (56.52%)	12 (52.17%)	14 (60.87%)	
Female	20 (43.48%)	11 (47.83%)	9 (39.13%)	
QOD	N/A	N/A	31.00 [14.50, 43.00]	
OCES	N/A	N/A	4.00 [2.00, 7.00]	
TDI	N/A	N/A	3.00 [0.00, 17.75]	
Threshold	N/A	N/A	0.00 [0.00, 2.75]	
Discrimination	N/A	N/A	2.00 [0.00, 6.00]	
Identification	N/A	N/A	3.00 [0.00, 9.00]	

¹ Median [IQR]; n (%). ² Wilcoxon rank sum test; Pearson's Chi-squared test. Note: N/A, not applicable; HC, healthy controls; CRS-OD, Chronic Rhinosinusitis with Olfactory Dysfunction; QOD, questionnaire of olfactory disorders; TDI, threshold, discrimination and identification.

Table 2. Comparison of olfactory bulb volume between groups.

Variable	CRS-OD N = 17	HC N = 17	p-value ²
Volume_R	40.00 (8.05)	46.83 (6.04)	0.012
Volume_L	39.65 (8.45)	46.75 (6.31)	0.016

¹ Mean (SD); ² p-values derived from general linear models (GLM).

ment. CRS-OD patients exhibited significantly smaller bilateral OB volumes compared to HCs ($p < 0.05$, Table 2).

Results of olfactory bulb measurements

The inter-rater reliability for OB volume delineation was 0.81, indicating a high level of agreement between the two raters. Bilateral OB volumes were significantly smaller in the CRS-OD group compared to HCs ($p < 0.05$).

Gray matter volume analysis

VBM analysis revealed significant gray matter volume reductions in CRS-OD patients compared to HCs, specifically in the right inferior frontal orbital gyrus, right parahippocampal gyrus, right hippocampus, bilateral thalamus, and bilateral putamen ($p < 0.05$, FDR corrected; Figure 2). Notably, OCES scores negatively correlated with the volume of the right putamen ($p = 0.044$, $r = -0.467$; Figure 3a), while QOD scores showed a negative correlation with the volume of the right hippocampus ($p = 0.007$, $r = -0.600$; Figure 3b).

Seed based FC analysis

Whole-brain FC analysis, using regions with significant volume

reductions as seed points, revealed decreased connectivity in CRS-OD patients between the left putamen and the left insula, right posterior cingulate, and right inferior frontal gyrus (Figure 4). Additionally, reduced FC was observed between the right putamen and the right mid-cingulate and precuneus, whereas increased FC was noted with the right superior occipital gyrus compared to HCs. However, no significant correlations were found between FC alterations and clinical outcomes. Apart from the bilateral putamen, no other regions showed significant FC differences.

Discussion

This study investigated structural and functional alterations in CRS-OD patients using multimodal MRI. CRS-OD patients exhibited significantly reduced OB volumes compared to HCs, suggesting that chronic inflammation leads to neural degeneration and diminished sensory input to the OB. Additionally, gray matter atrophy and disrupted FC in sensory-integration networks were observed, indicating the widespread neural impact of CRS-OD. The correlations between gray matter volume reductions, clinical assessments, and OB morphology further underscore the interplay between peripheral and central olfactory dysfunction, highlighting the broader implications of CRS-OD on sensory integration and cognitive-emotional processing.

Gray matter alterations and their broader implications in CRS-OD

We observed significant gray matter volume reductions in olfactory-related regions such as the orbitofrontal cortex and hippocampus. These findings are consistent with previous studies reporting structural changes in central olfactory processing areas in the context of chronic olfactory dysfunction⁽³¹⁾. More-

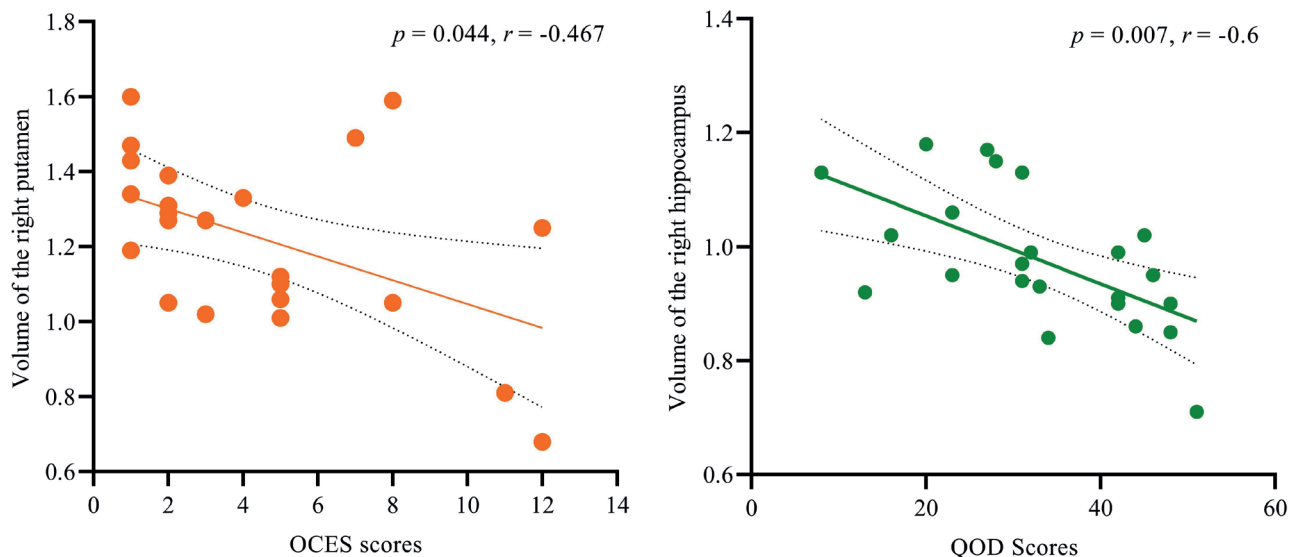


Figure 3. Correlation Between Brain Volume and Clinical Scores in CRS-OD Patients. A) A significant negative correlation was observed between the right putamen volume and OCES scores ($p=0.044$, $r=-0.467$). B) A significant negative correlation was found between the right hippocampal volume and QOD scores ($p=0.007$, $r=-0.600$). Regression lines with 95% confidence intervals are displayed. CRS-OD, Chronic rhinosinusitis with olfactory dysfunction; OCES, Olfactory-Evoked Cognitive Score; QOD, Questionnaire of Olfactory Disorders.

over, the observed correlation between hippocampal volume and QOD scores may reflect potential cognitive involvement in CRS-OD, although further studies are needed to confirm this relationship.

Notably, we also identified reductions in the bilateral thalamus and putamen, which have not been consistently reported in previous CRS-OD studies. The observed negative correlation between the right putamen volume and OCES scores⁽³²⁾, suggests a possible role of this region in olfactory-related sensory integration and emotional processing. However, these interpretations should be considered exploratory given the limited information on the duration and severity fluctuation of olfactory dysfunction in our cohort. Taken together, our results not only confirm previously reported neuroanatomical alterations in CRS-OD^(3,12), but also extend these observations to additional brain regions, emphasizing the need for further investigation into the broader neural consequences of CRS-OD.

Functional connectivity alterations

FC analysis revealed decreased connectivity between the putamen and key regions involved in sensory integration and cognitive control, including the left insular cortex, right posterior cingulate cortex, and right inferior frontal gyrus. Furthermore, the right putamen showed reduced connectivity with the right mid-cingulate cortex and precuneus. These findings suggest disruptions in neural networks crucial to olfactory and cognitive function, which may reflect the broader impact of CRS-OD beyond primary olfactory pathways.

In contrast, the increased FC between the right putamen

and the right superior occipital gyrus may reflect a potential compensatory or maladaptive sensory integration mechanism. Recent studies have likewise reported altered occipital network connectivity in CRS-OD patients⁽²⁶⁾, suggesting that visual cortices may participate in cross-modal reorganization in response to olfactory dysfunction. Such neuroplastic changes have also been documented in other sensory-deprived conditions, including blindness and hearing loss, where visual or auditory cortices are recruited to compensate for the impaired modality^(33,34). Nonetheless, further studies incorporating behavioral assessments and longitudinal follow-up are warranted to clarify the functional significance of this finding.

Olfactory bulb atrophy in CRS-OD

In our study, CRS-OD patients exhibited significantly smaller bilateral OB volumes compared to HCs, consistent with prior reports of OB atrophy in chronic olfactory impairment^(35,36). These findings underscore the vulnerability of the OB to chronic inflammation, which likely leads to neural degeneration, reduced sensory input, and impaired neurogenesis, ultimately resulting in volume loss. This cumulative impact of prolonged inflammation emphasizes the progressive atrophic changes of the OB observed in chronic conditions such as CRS-OD. While transient hypertrophy may occur during the early stages of inflammation due to compensatory mechanisms, persistent inflammation appears to dominate in advanced stages, leading to progressive atrophy⁽³⁷⁾.

Understanding the temporal dynamics of OB changes in CRS-OD is critical for improving clinical management. Future studies

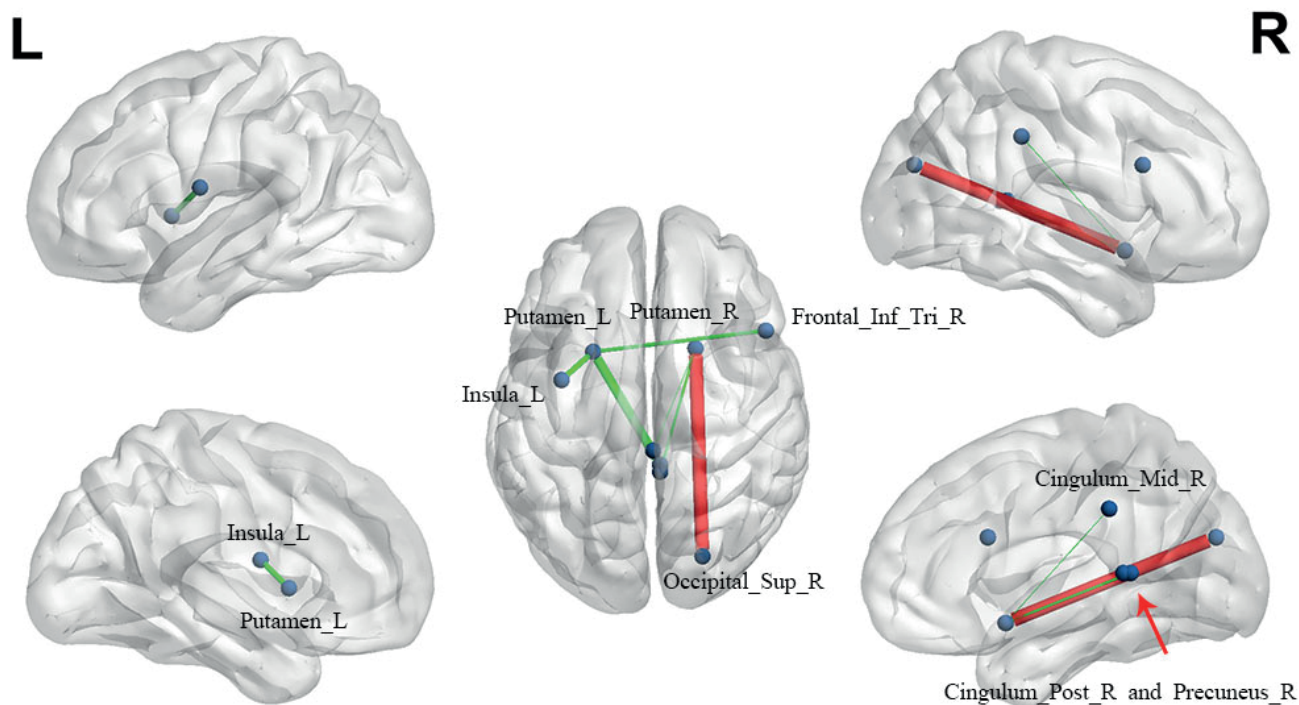


Figure 4. FC Analysis of the Bilateral Putamen in CRS-OD Patients. FC analysis revealed bilateral putamen exhibited significant connections with multiple brain regions. Green lines indicate decreased FC, whereas red lines indicate increased FC. The thickness of the lines represents the strength of the connectivity. FC, Functional connectivity; CRS-OD, Chronic rhinosinusitis with olfactory dysfunction.

should investigate how OB atrophy correlates with disease duration, severity, and treatment response, providing a foundation for targeted therapeutic interventions aimed at preserving olfactory function.

Study limitations

This study has several limitations. The relatively small sample size and cross-sectional design restrict causal inferences and hinder the ability to observe neuroplastic changes over time. Additionally, the findings, while significant, are derived from a single-center cohort, which may limit their generalizability to broader populations. Multi-center studies with larger and more diverse cohorts are necessary to validate these results and enhance their applicability. Furthermore, longitudinal investigations are essential to capture the dynamic relationship between structural and functional brain changes and clinical outcomes, offering deeper insights into the mechanisms underlying olfactory dysfunction and potential recovery pathways.

Conclusion

Our findings provide novel evidence of both structural and functional brain alterations in CRS-OD that extend beyond the primary olfactory regions. These results underscore the complex central neural alterations in CRS-OD and highlight the need for

future longitudinal and mechanistic studies to further elucidate its neural basis and potential clinical implications.

Acknowledgements

The authors sincerely thank the patients who participated in this study and the staff of the Department of Radiology and Otolaryngology for their invaluable support. The authors gratefully acknowledge Ms. Carly Skudin (MRI Research Institute, Department of Radiology, Weill Cornell Medicine) for her valuable assistance in language editing and manuscript polishing.

Authors' contributions

CZ and YZ conceptualized and designed the study, developed the implementation plan, and drafted the initial manuscript. YZ and ZT were responsible for patient recruitment, clinical data collection, and subsequent data analysis. QW contributed to the study design and provided critical insights into data interpretation. CJ, JS, XW, WZ, and TC contributed to the acquisition and processing of imaging data, as well as performing image analysis. KX oversaw project administration and conducted a comprehensive review of the manuscript. YZ and KX jointly supervised the study and played a pivotal role in the critical revision of the manuscript. All authors have read and approved the final version of the manuscript.

Funding

This research was supported by the Research Project of Elderly Health in Jiangsu Province (No. LKM2023014), the Health Committee of Jiangsu Province (No. H2023134), and the Paired Assistance Scientific Research Project by The Affiliated Hospital of Xuzhou Medical University (No. SHJDBF2024216). Additional support was provided by the Open Project of Key Laboratories

in Colleges and Universities in Jiangsu Province (No. XZ-SYSKF2020012) and the Key R&D Plan (Social Development) Project of Xuzhou Science and Technology Bureau (No. KC22240).

Conflicts of interest

None.

References

1. Mattos JL, Schlosser RJ, Storck KA, Soler ZM. Understanding the relationship between olfactory-specific quality of life, objective olfactory loss, and patient factors in chronic rhinosinusitis. *Int Forum Allergy Rhinol.* 2017; 7(7): 734-740.
2. Taha T, Megahed AA, Taha MS, et al. Diffusion tensor imaging: a smart move to olfactory pathway imaging; comparative study of chronic sinonasal polyposis patients and normal control. *Egypt J Radiol Nucl Med.* 2020; 51:34.
3. Ma Y, Jiang J, Wu Y, et al. Abnormal functional connectivity of the core olfactory network in patients with chronic rhinosinusitis accompanied by olfactory dysfunction. *Front Neurol.* 2023; 14: 2023:1295556.
4. Zhang L, Association between peripheral eosinophilia, JESREC score, and olfactory dysfunction in patients with chronic rhinosinusitis. *Front Immunol.* 2024; 15: 2024:1334656.
5. Whitcroft KL, Altundag A, Balungwe P, et al. Position paper on olfactory dysfunction: 2023. *Rhinology.* 2023; 61(33): 1-108.
6. Hummel T, Whitcroft KL, Andrews P, et al. Position paper on olfactory dysfunction. *Rhinology.* 2016; 56(1): 1-30.
7. Alobid I, Barroso B, Calvo C, Ferrario MG, Sastre J. Effect of different therapeutic strategies on olfactory outcomes in patients with chronic rhinosinusitis with nasal polyps: a systematic review. *J Investig Allergol Clin Immunol.* 2024; 34(4): 218-224.
8. Chen M, Reed RR, Lane AP. Chronic Inflammation Directs an Olfactory Stem Cell Functional Switch from Neuroregeneration to Immune Defense. *Cell Stem Cell.* 2019; 25(4): 501-513 e505.
9. Yee KK, Pribitkin EA, Cowart BJ, et al. Neuropathology of the olfactory mucosa in chronic rhinosinusitis. *Am J Rhinol Allergy.* 2010; 24(2): 110-120.
10. Victores AJ, Chen M, Smith A, Lane AP. Olfactory loss in chronic rhinosinusitis is associated with neuronal activation of c-Jun N-terminal kinase. *Int Forum Allergy Rhinol.* 2018; 8(3): 415-420.
11. Kern RC. Chronic sinusitis and anosmia: pathologic changes in the olfactory mucosa. *Laryngoscope.* 2000; 110(7): 1071-1077.
12. Han P, Whitcroft KL, Fischer J, et al. Olfactory brain gray matter volume reduction in patients with chronic rhinosinusitis. *Int Forum Allergy Rhinol.* 2017; 7(6): 551-556.
13. Whitcroft KL, Cuevas M, Andrews P, Hummel T. Monitoring olfactory function in chronic rhinosinusitis and the effect of disease duration on outcome. *Int Forum Allergy Rhinol.* 2018; 8(7): 769-776.
14. Kennedy DW. Olfactory loss in chronic rhinosinusitis. *Int Forum Allergy Rhinol.* 2017; 7(6): 549-550.
15. Hema V, Rebekah G, Kurien R. Reversibility of mucociliary clearance and olfaction impairment following endoscopic sinus surgery: a prospective observational study. *J Laryngol Otol.* 2021; 135(2): 147-152.
16. Sánchez-Vallecillo MV, Fraire ME, Baena-Cagnani C, Zernotti ME. Olfactory dysfunction in patients with chronic rhinosinusitis. *Int J Otolaryngol.* 2012; 2012: 327206.
17. Seubert J, Freiherr J, Djordjevic J, Lundström JN. Statistical localization of human olfactory cortex. *Neuroimage.* 2013; 66: 333-342.
18. Kropf E, Syan SK, Minuzzi L, Frey BN. From anatomy to function: the role of the somatosensory cortex in emotional regulation. *Braz J Psychiatry.* 2019; 41(3): 261-269.
19. Rolls ET. The orbitofrontal cortex and reward. *Cereb Cortex.* 2000; 10(3): 284-294.
20. Cavanna AE, Trimble MR, The precuneus: a review of its functional anatomy and behavioural correlates. *Brain.* 2006; 129(Pt 3): 564-583.
21. Zhang C, Wu C, Zhang H, et al. Disrupted resting-state functional connectivity of the nucleus basalis of Meynert in Parkinson's Disease with mild cognitive impairment. *neuroscience.* 2020; 442: 228-236.
22. Fox MD, Raichle ME. Spontaneous fluctuations in brain activity observed with functional magnetic resonance imaging. *Nat Rev Neurosci.* 2007; 8(9): 700-711.
23. Biswal B, Yetkin FZ, Haughton VM, Hyde JS. Functional connectivity in the motor cortex of resting human brain using echo-planar MRI. *Magn Reson Med.* 1995; 34(4): 537-541.
24. Zhang Z, Wu Y, Luo Q, et al. Regional homogeneity alterations of resting-state functional magnetic resonance imaging of chronic rhinosinusitis with olfactory dysfunction. *Front Neurosci.* 2023; 17: 1146259.
25. Dekeyser A, Huart C, Hummel T, Hox V. Olfactory loss in rhinosinusitis: mechanisms of loss and recovery. *Int J Mol Sci.* 2024; 25(8): 4460.
26. Kuang H, Hong S, Chen Y, et al. Altered internetwork functional connectivity and graph analysis of occipital regions in patients with chronic rhinosinusitis accompanied by olfactory dysfunction. *Sci Rep.* 2025; 15(1): 10951.
27. Fokkens WJ, Lund VJ, Hopkins C, et al. European Position Paper on Rhinosinusitis and Nasal Polyps 2020. *Rhinology.* 2020 Feb 20:58(Suppl S29):1-464.
28. Feng M, Wen H, Li J, Lv H, Cho J, Guo LF. Editorial: Neuroimaging of brain structure-function coupling mechanism in neuropsychiatric disorders. *Front Neurosci.* 2023; 17: 1270645.
29. Feng G, Zhuang Y, Yao F, Ye Y, Wan Q, Zhou W. Development of the Chinese smell identification test. *Chem Senses.* 2019; 44(3): 189-195.
30. Yan CG, Wang XD, Zuo XN, Zang YF. DPABI: data processing & analysis for (resting-state) brain imaging. *Neuroinformatics.* 2016; 14(3): 339-351.
31. Bitter T, Gudziol H, Burmeister HP, Mentzel HJ, Guntinas-Lichius O, Gaser C. Anosmia leads to a loss of gray matter in cortical brain areas. *Chem Senses.* 2010; 35(5): 407-415.
32. Ghandili M, Munakomi S. Neuroanatomy, Putamen, in *StatPearls.* Treasure Island (FL) ineligible companies (StatPearls Publishing, 2022).
33. Manes JL, Tjaden K, Parrish T, et al. Altered resting-state functional connectivity of the putamen and internal globus pallidus is related to speech impairment in Parkinson's disease. *Brain Behav.* 2018; 8(9): e01073.
34. Ghaziri J, Fei P, Tucholka A, et al. Resting-state functional connectivity profile of insular subregions. *Brain Sci.* 2024; 14(8): 742.
35. Rombaux P, Mouraux A, Bertrand B, Nicolas G, Duprez T, Hummel T. Olfactory function and olfactory bulb volume in patients with postinfectious olfactory loss. *Laryngoscope.* 2006; 116(3): 436-439.
36. Hummel T, Urbig A, Huart C, Duprez T, Rombaux P. Volume of olfactory bulb and depth of olfactory sulcus in 378 consecutive patients with olfactory loss. *J Neurol.* 2015; 262(4): 1046-1051.
37. Haehner A, Rodewald A, Gerber JC, Hummel T. Correlation of olfactory function with changes in the volume of the human olfactory bulb. *Arch Otolaryngol Head Neck Surg.* 2008; 134(6): 621-624.

Corrected Proof

Zhang et al.

Kai Xu	Yunpeng Zang
Department of Radiology	Department of Otolaryngology
Affiliated Hospital of Xuzhou Medical	Affiliated Hospital of Xuzhou Medical
University	University
No.99, Huaihai West Road	No.99, Huaihai West Road
Quanshan District	Quanshan District
Xuzhou, 221000	Xuzhou, 221000
Jiangsu	Jiangsu
P.R. China	P.R. China
Tel: +86-051685806538	E-mail: yunpengzang23@163.com
E-mail: xukai@xzhmu.edu.cn	

Chao Zhang¹, Qi Wang¹, Canran Jiang¹, Zhenni Tian³, Jingyun Sha¹,
Xiao Wang¹, Wanrong Zhou¹, Teng Cui¹, Yunpeng Zang^{2,*}, Kai Xu^{1,*}

Rhinology 64: 1, 0 - 0, 2026

<https://doi.org/10.4193/Rhin25.096>

Received for publication:

February 17, 2025

Accepted: August 6, 2025

¹ Department of Radiology, Affiliated Hospital of Xuzhou Medical University, Xuzhou, Jiangsu, P.R. China

² Department of Otolaryngology, Affiliated Hospital of Xuzhou Medical University, Xuzhou, Jiangsu, P.R. China

³ The first clinical medical college of Xuzhou Medical University, Xuzhou, Jiangsu, China

Associate Editor:

Basile Landis